Geosci. Model Dev. Discuss., 6, 5595–5644, 2013
www.geosci-model-dev-discuss.net/6/5595/2013/
doi:10.5194/gmdd-6-5595-2013


Geoscientific Model Development Discussions
Open Access



# Turbulent transport, emissions, and the role of compensating errors in chemical transport models

**P. A. Makar[1], R. Nissen[2], A. Teakles[2], J. Zhang[1], Q. Zheng[1], M. D. Moran[1], H. Yau[2], and C. diCenzo[2,*]**

[1]Air Quality Research Division, Environmental Science and Technology Directorate, Environment Canada, M3H 5T4 Toronto, Ontario, Canada
[2]Air Quality Science Unit, Pacific and Yukon Region, Environment Canada, Vancouver, B.C., Canada
[*]retired

Received: 22 September 2013 – Accepted: 25 September 2013 – Published: 7 November 2013

Correspondence to: P. A. Makar (paul.makar@ec.gc.ca)

Published by Copernicus Publications on behalf of the European Geosciences Union.

## Abstract

The balance between turbulent transport and emissions is a key issue in understanding the formation of $O_3$ and $PM_{2.5}$. Discrepancies between observed and simulated concentrations for these species are often ascribed to insufficient turbulent mixing, particularly for atmospherically stable environments. This assumption may be inaccurate – turbulent mixing deficiencies may explain only part of these discrepancies, while the timing of primary $PM_{2.5}$ emissions may play a much more significant role than previously believed. In a study of these issues, two regional air-quality models, CMAQ and AURAMS, were compared against observations for a domain in north-western North America. The air quality models made use of the same emissions inventory, emissions processing system, meteorological driving model, and model domain, map projection and horizontal grid, eliminating these factors as potential sources of discrepancies between model predictions. The initial statistical comparison between the models against monitoring network data showed that AURAMS' $O_3$ simulations outperformed those of CMAQ, while CMAQ outperformed AURAMS for most $PM_{2.5}$ statistical measures. A process analysis of the models revealed that the choice of an a priori cut-off lower limit in the magnitude of vertical diffusion coefficients in each model could explain much of the difference between the model results for both $O_3$ and $PM_{2.5}$. The use of a larger value for the lower limit in vertical diffusivity was found to create a similar $O_3$ and $PM_{2.5}$ performance in AURAMS as was noted in CMAQ (with AURAMS showing improved $PM_{2.5}$, yet degraded $O_3$, and a similar time series as CMAQ). The differences between model results were most noticeable at night, when the use of a larger cut-off in turbulent diffusion coefficients resulted in an erroneous secondary peak in predicted night-time $O_3$. Further investigation showed that the magnitude, timing and spatial allocation of area-source emissions could result in improvements to $PM_{2.5}$ performance with minimal $O_3$ performance degradation. The use of a relatively high cut-off in diffusion may in part compensate for erroneously high night-time $PM_{2.5}$ emissions, but at the expense of increasing model error in $O_3$. While the strength of turbulence plays a key role in $O_3$





GMDD
6, 5595–5644, 2013

and $PM_{2.5}$ formation, more accurate primary $PM_{2.5}$ temporal emissions data may be needed to explain observed concentrations, particularly in urban regions.

## 1 Introduction

Several studies within the last decade have shown the value of the comparison of multiple air-quality models to a common suite of observations. Two studies made use of data collected during the International Consortium for Atmospheric Research on Transport and Transformation/New England Air–Quality Study (ICARTT/NEAQS). McKeen et al. (2005) used seven air-quality forecast models to show that ensemble $O_3$ forecasts based on the 7-member mean and the 7-member median had better temporal correlation to the observed daily maximum 1 h average and maximum 8 h average than any individual model, for a domain covering the eastern USA and south-eastern Canada. The usefulness of uncorrected ensembles was shown to be limited by positive biases in $O_3$ inherent to all seven ensemble members. The best method of bias correction was found to be model dependent. In a subsequent examination for the same region and period using the same models, McKeen et al. (2007) found that $PM_{2.5}$ forecasts had similar correlation, lower bias and better skill compared to the ozone forecasts. A feature of this work was an analysis of diurnal variability – most models failed to reproduce the observed diurnal cycle of $PM_{2.5}$ concentrations at urban and suburban monitor locations. This error in the predicted diurnal cycle was most pronounced in the transition period between night and early morning. Four of the models showed greater diurnal $PM_{2.5}$ variability than was observed, with differences in emissions inventories, the PBL parameterizations employed, and the timing of the predicted morning growth of the PBL all postulated as factors affecting the model performance. The work also identified insufficient model nocturnal mixing as a key factor in low surface sulphate predictions (due to insufficient vertical turbulent transport of sulphate aloft to the surface), and in excessively high predicted surface elemental carbon and $NO_x$ predictions (due to insufficient turbulent transport of these species emitted at the surface to higher model levels). These effects were noted for the on-line Weather Research and Forecasting – CHEMistry (WRF-CHEM) model, which de facto makes use of the turbulence parameterizations inherent in the driving meteorology. Subsequent model ensemble work for the second Texas Air Quality Study (TexAQS II, McKeen et al., 2009), showed that the relationship between model emissions levels and concentration difference ratios was approximately linear (to within 25 %), with improvements to emissions inventories through the use of continuous emissions monitors and updated mobile emissions resulting in better agreement with observations. The study also noted that despite ratios of $PM_{2.5}$ to $NO_y$ matching observations, underpredictions of $PM_{2.5}$ organic carbon suggested that this might be a result of compensating errors, with excessive model primary $PM_{2.5}$ making up for the absence of sufficient model secondary organic aerosol formation.

Multiple model intercomparisons were expanded to include both North American and European domains in the Air-Quality Model Evaluation International Initiative (AQMEII, Galmarini and Rao, 2011), with 23 modelling groups providing annual simulations on either or both of these domains. In a further refinement of ensemble forecasting techniques, researchers participating in this study found that full ensemble mean predictions could be outperformed by subset ensembles of model members selected for an optimal set of error characteristics (Solazzo et al., 2012a). Predictions of PM were also investigated; (Solazzo et al., 2012b) showed that all of the models employed underestimated $PM_{10}$, with better estimates for $PM_{2.5}$, though no model consistently matched $PM_{2.5}$ observations for the period and stations simulated. While anthropogenic emissions were prescribed as part of the intercomparison, differences in natural emissions of some PM components such as sea-salt were shown to have a significant impact on some model results. The member of the ensemble which made use of a different inventory from that prescribed in the study protocol was shown to have significantly different (factor of four lower) $PM_{10}$ emissions than the other models, showing the potential importance of inventory accuracy on $PM_{10}$ predictions. Large differences in particulate deposition rates despite similar theoretical approaches for deposition were attributed





GMDD
6, 5595–5644, 2013

to differences in the characterization of surface properties and near-surface meteorology, with the fractional bias of the $PM_{10}$ seasonal concentration varying by up to 60 % depending on which deposition module was used within a single model (Nopmongcol et al., 2012). Models with the highest deposition rates of $PM_{2.5}$ were also found to have the most significant negative biases in $PM_{2.5}$ concentrations. Model performance for $PM_{10}$ was better in the summer months than in winter, with difficulties in the accurate simulation of very stable boundary layers in the winter being a possible cause of model prediction errors. Most models underestimated the amplitude of the diurnal cycle of $PM_{10}$ as well as being biased low. The inorganic $PM_{2.5}$ components were better simulated than the organics, demonstrating the ongoing problem with accurate simulations of organic aerosol. While the study did not examine or compare the models' individual chemical process parameterizations in detail, a conclusion of the work was that the details of those parameterizations play a pivotal role in model performance, despite similarities in the overall schemes employed.

One two-model intercomparison attempted to eliminate some of the sources of model prediction variability by prescribing additional model inputs aside from the meteorology. Smyth et al. (2009) used the same emissions inventory, emissions processing system, meteorological driver, North American domain, and map projection, to eliminate these factors as sources of possible differences between the two models compared (CMAQ and AURAMS). Despite these similarities, some significant differences in model performance were noted. AURAMS had a normalized mean bias (NMB) for hourly $O_3$ that was less than half of that for CMAQ (21 % vs. 46 %, respectively), while both models had similar normalized mean errors (NME, 47 % vs. 54 %). The larger NMB errors for CMAQ were shown to be related to its inability to predict the observed night-time $O_3$ minima. Both models' $PM_{2.5}$ predictions were biased low (−10 % and −65 %, respectively), though both had similar NME $PM_{2.5}$ scores, with much of the reduced $PM_{2.5}$ bias in AURAMS being the result of high sea-salt predictions in the latter model. Both models underpredicted the organic fraction of $PM_{2.5}$. The study noted the potential difficulties in the systematic assessment of individual science processes on the model results, due to the complexity and interconnected nature of the science processes.

The above body of work demonstrates both the value of model evaluation and intercomparisons and the corresponding difficulties. Conducting multi-model studies requires a considerable investment in the preparation and evaluation of model fields. A common finding of studies such as those described above is that differences in the performance between the different models lies in their process parameterizations, yet process-level studies comprise an additional level of complexity, and are consequently not always part of large-scale multi-model comparisons with observations. However, when significant differences are found between models employing harmonized input fields, process-level evaluations may provide valuable information on the reasons underscoring model performance. In the work that follows, we describe a process-level comparison of the CMAQ and AURAMS models on a more limited regional domain. The emissions inventories, emissions processing system, model domain, map projection and the driving meteorology were held in common for the two models, allowing two key factors in model performance to be identified: the accuracy of inputs used to create model emissions, and the models' assumptions regarding turbulent diffusion.

## 2 Model description

The two models employed in this process study are the Community Multiscale Air Quality (CMAQ, version 4.6) and A Unified Regional Air-quality Modelling System (AURAMS, v1.4.2). A detailed description of the two models may be found in Smyth et al. (2009), and updates to the AURAMS model (Gong et al., 2006) subsequent to that time may be found in Kelly et al. (2012), while CMAQ v4.6 is also described in Pleim et al., (2006). Here, we note some of the main features of the two models, with reference to Table 1.

Both models made use of meteorology from the Global Environmental Multiscale weather forecast model (GEM, v3.2.2, Côté et al., 1998); GEM simulations were carried out on a rotated latitude/longitude grid, for the period 15 July through 15 August 2005 in a series of overlapping 30 h simulations for a North American domain, with 0.1375° horizontal grid spacing (approximately 15 km), starting from model analysis files at 00:00 UTC on each day. The first six hours of each of these simulations were discarded as "spin-up" in order to allow the model's cloud variables to reach a steady-state. The remaining hours (6 through 30) were retained for use as a continuous sequence of air-quality model meteorological input. Two days of spin-up time was employed in the meteorological models – this being sufficient for air parcels starting at the upwind boundary to cross the downwind boundary of this relatively small simulation domain.

The meteorological files were interpolated to the 12 km grid spacing air-quality model domain (Fig. 1a, inset white region, and Fig. 1b which also shows the air-quality model grid along with observation network stations). The domain encompasses the coastal northwestern USA and coastal southwestern Canada. Several unique features of this domain should be noted, as are described in more detail in previous work by Steyn et al., (2013) and Ainslie et al., (2013): (1) unlike many locations in North America, the upwind boundary condition of the domain consists of relatively "clean" air associated with trans-pacific transport; (2) the terrain is mountainous – previous work (Brook et al., 2004) suggests that recirculation events in which aged air carried aloft with upslope flow is returned to the surface over the ocean, allowing accumulation of pollutants; and (3) the boundaries between $NO_x$ and volatile organic compound sensitivity in the region have been changing over time, indicating that the region contains markedly different chemical regimes, depending on location (Ainslie et al., 2013).

While the models employ the same horizontal domain map projection and grid, they differ in their vertical coordinate and number of levels. AURAMS uses a Gal–Chen coordinate system with 27 layers and a model top at 30 km, while CMAQ uses a sigma coordinate system with 15 layers and a model top at approximately 15 km. The thickness of the model layers differs, but tests in which the AURAMS layer thicknesses were imported into CMAQ had a negligible impact on CMAQ performance. Both models make use of their default boundary conditions; for AURAMS1.4.2, these vary with





GMDD
6, 5595–5644, 2013

season for some species, and for $O_3$ an adjustment of climatological boundary conditions in response to the local tropopause height is employed (Makar et al., 2010). While the upwind boundary conditions of the models differ, they both describe relatively clean conditions, as is appropriate for the upwind condition of the domain. A comparison of the $PM_{2.5}$ and $O_3$ predictions of the models over the Pacific (upwind boundary condition) in relative to the urban regions shows that the changes associated with urban local chemistry and dynamics are an order of magnitude greater than the variations that may be observed in the upwind boundary region of the model. The effects described below are thus the result of local changes in the models' respective responses to the emissions, rather than to upwind boundary conditions.

Both models made use of the same satellite-derived land-use data as driving conditions for gas and particle deposition, but the algorithms employed differ, with AURAMS making use of the parameterizations of Zhang et al. (2001, 2002) and CMAQ employing the model of Xiu and Pleim (2000).

Both models made use of the same emissions inventories. Environment Canada 2006 and US Environmental Protection Agency (EPA) 2005 anthropogenic inventories were combined for this work, and both models made use of the BEIS3.0.9 biogenic emissions algorithms and BELD3 land-use data. The gas-phase chemical mechanism employed in AURAMS is the ADOM-II mechanism (Stockwell and Lurmann, 1989), while CMAQ made use of the SAPRC-99 mechanism (Carter et al., 2000a, b). The models have a similar particulate matter chemical speciation, however, the particle size distribution in AURAMS makes use of a 12-bin sectional approach while CMAQ uses a 3-mode modal approach. The emissions in both models thus had to be speciated for that model's chemical mechanism and particle size distribution.

Emissions for both models were generated using the Sparse Matrix Operator Kernal Emissions processing system (SMOKE; Houyoux et al., 2000; CEP, 2003). Emissions processing systems such as SMOKE make use of input emissions inventories which usually comprise annual emissions totals for different sources over a geopolitical region such as state/province/county/municipality. These annual values are distributed within





GMDD
6, 5595–5644, 2013



Title Page
Abstract | Introduction
Conclusions | References
Tables | Figures
◂◂ | ▸▸
◂ | ▸
Back | Close
Full Screen / Esc
Printer-friendly Version
Interactive Discussion

the geopolitical region using spatial disaggregation data – gridded maps of the expected spatial distribution of pollutants, derived from surrogate fields believed to reflect the distribution of the emitting activities. The emissions are also required by the models on an hourly basis, hence the annual emissions must also be distributed over time. Temporal allocations are required to split the annual emissions into month-of-year, day-of-week within each month, and hour-of-day within each day. The accuracy of the gridded emissions used as model input will depend on the extent to which these assigned spatial and temporal fields accurately reflect the true temporal and spatial distributions, as well as on the annual total geopolitically-distributed emissions. Unfortunately, the available spatial surrogate fields are severely outnumbered by the number of emitting activities, with thousands of source types typically being represented by a few hundred surrogates (here, a total of 170 surrogates were used). Similarly, the temporal profiles used for an emitting activity are often best guess approximations which are not based on observed monthly/day of week/hour of day emissions for any given emitting activity to which they are assigned. The assignments for spatial and temporal disaggregation of annual emissions are of crucial importance in determining the resulting model accuracy for circumstances when the spatial and temporal distribution of emissions have a significant impact on local concentrations (i.e. close to the sources as opposed to further downwind). The impact of the choice of spatial and temporal disaggregation data are examined in several scenario simulations in the Sect. 4.2.

The models differ in the approach taken for vertical diffusion. AURAMS uses diffusion coefficients for heat and moisture from the driving meteorological model along with a fully implicit Laasonen approach for the discretization of the diffusion equation (c f. Richtmyer, 1994). CMAQ calculates diffusion coefficients based on the driving meteorological model's values for the temperature, wind speed, total liquid water content, specific humidity, surface pressure, friction velocity and height of the boundary layer (Pleim, 2007). Numerical solution of the diffusion equation is carried out in CMAQ using the Crank–Nicholson discretization (cf. Richtmyer, 1994). Both models subsequently employ a lower limit to their diffusion coefficients, with this "floor" in diffusion in AURAMS being set to 0.1 $m^2 s^{-1}$, and in our CMAQ simulations this was set to 1.0 $m^2 s^{-1}$. Other options available for the use of this version of CMAQ include using higher values of the diffusion coefficient lower limit over urban areas (2.0 $m^2 s^{-1}$), and lower values over rural areas (0.5 $m^2 s^{-1}$). The choice of a specific lower limit has a significant impact on model performance (cf. CMAS, 2006). However, the analysis which follows suggests that the underlying assumption (that these performance problems are primarily associated with inadequate turbulence parameterizations) is inadequate to explain the discrepancies between observed and predicted $O_3$ and $PM_{2.5}$.

The model results were evaluated using hourly $O_3$ and $PM_{2.5}$ data from four monitoring networks (Air Quality System; AQS, Canadian Air and Precipitation Monitoring Network; CAPMoN, Clean Air Status and Trends Network; CASTNET, and National Air Pollution Surveillance program; NAPS). Model values are instantaneous hourly in the case of CMAQ, while AURAMS output are hour-ending averages of 15 min output. Station locations are shown in Fig. 1b, with five stations in the Lower Fraser Valley in Fig. 1c. The Lower Fraser Valley contains a large proportion of the population of the province of British Columbia; portions of our analysis examine model performance in this sub-region in detail. AURAMS output was available on a 15 min timestep, while CMAQ output was hourly; the AURAMS values were averaged to create hourly values for comparison to the observations. An analysis package using the R programming language (R Development Core Team, 2010) was created for model evaluation making use of the "openair" R package (Carslaw and Ropkins, 2011). The output package of AURAMS 1.4.2 includes output at station locations during model run-time, while CMAQ output was derived from output netCDF files using the work of Pierce (2010). Visualization packages utilized in creating the graphical display of analyzed fields included hexbin (Carr/Lewin-Koh and Maechler, 2010), and Lattice (Deepayan, 2008).





GMDD
6, 5595–5644, 2013

## 3 Model simulations

Nine model simulations were carried out, in order to evaluate the impact of improvements to model algorithms, improvements and sensitivity to emissions inputs, and the impact of changes to the value of the lower limit for eddy diffusivity (Table 2). The first two of these are unmodified CMAQ and AURAMS simulations; the "base case" scenarios (CMAQ1 and AURAMS1). As will be noted below, these scenarios showed a marked difference between the models with regards to their performance for $PM_{2.5}$ and $O_3$. The base case scenarios are followed by several process and emissions input related scenarios: AURAMS1b – a scenario in which several process improvements were added to the AURAMS model and evaluated as a package; CMAQ2 and AURAMS2; in which the impact of improved emissions data were evaluated using both models; and four subsequent AURAMS simulations (AURAMS3 through AURAMS6), which investigated the AURAMS model sensitivity to further emissions changes and the use of a larger cut-off in diffusion than was used in the base-case model. These scenarios and the rationale for their execution will be described below.

## 4 Results

### 4.1 Initial comparison and analysis

The statistical measures used in our analysis are presented in Table 3. The resulting analyses of the base case $O_3$ and $PM_{2.5}$ simulations from each model are summarized in the first two columns of Table 4. Table 4a and b show the statistical scores for the entire grid, and Table 5 shows the $PM_{2.5}$ scores for the five stations in the Lower Fraser Valley. The initial results showed a substantial difference in model performance: AURAMS outperformed CMAQ for hourly ozone for the entire grid statistics (Table 4a), for all Canadian stations aside from tying with CMAQ for correlation coefficient (not shown), and for the majority of the statistical metrics for the Lower Fraser Valley (not





GMDD
6, 5595–5644, 2013

shown). This was a marked contrast from the earlier North American domain comparison by Smythe et al. (2009), where AURAMS outperformed CMAQ for $O_3$ mean bias, normalized mean bias, mean error and normalized mean error, while CMAQ outperformed AURAMS for correlation coefficient. Previous work with CMAQ for simulations in the same region for a period in August of 2001 had significantly better $O_3$ performance for NMB and NME than found here (Smyth et al., 2006: 13 % and 51 %, respectively, vs. 75 % and 82 % in the current work). CMAQ simulations by Steyn et al. (2013) for the region for specific short episodes in 2006, 2001, 1995, and 1985 reported NME values ranging from 43 % to 79 %, and NMB from −12 % to 64 %.

$PM_{2.5}$ scores in the current work were mixed, with CMAQ outperforming AURAMS across the grid (Table 4b) for minimum, *y* intercept, correlation coefficient, mean absolute error, mean squared error, root mean squared error and normalized mean error, and AURAMS outperforming CMAQ for mean, maximum, slope, mean bias and normalized mean bias. CMAQ outperformed AURAMS for $PM_{2.5}$ at Canadian stations for all scores aside from maximum and slope (not shown), while the Lower Fraser Valley performance (Table 5) was mixed, with scores split between the models.

An examination of time series of $O_3$ and $PM_{2.5}$ at the Vancouver airport station (Fig. 2 depicts a portion of the total time series for clarity; the depicted model behaviour occurs throughout the simulation period) shows the marked differences between the models in comparison to observations, as well as providing a potential physical and chemical explanation for the differences. CMAQ tended to overpredict daytime $O_3$ maxima, and invariably created a night-time secondary maximum in $O_3$ that is absent in the observations (Fig. 2a). AURAMS' $O_3$ time series more closely followed observations than those of CMAQ, though night-time minima were sometimes lower in the model than in the observations. The relative performance of the models is clearly reversed for $PM_{2.5}$ (Fig. 2b), with both models usually capturing the timing of the night-time peak $PM_{2.5}$ levels, but AURAMS greatly overestimated their magnitude relative to CMAQ.

The timing of the two models' respective positive biases in ozone and particulate matter helps explain these results. Both the CMAQ secondary ozone maxima and the

AURAMS $PM_{2.5}$ over-predictions occur *at night*. In an urban region at night, the dominant ozone chemical process is usually the destruction of ozone through titration by NO, the predicted surface concentrations of which were higher in AURAMS than in CMAQ. The composition of $PM_{2.5}$ at night in an urban location can be expected to be dominated by the primary components of particulate matter, given that the oxidation processes that lead to secondary aerosol formation dominate during the day. This was confirmed via a check of the time series for AURAMS' speciated $PM_{2.5}$ for the same period as Fig. 2 (not shown): the primary $PM_{2.5}$ species dominated the $PM_{2.5}$ mass during these periods of high positive $PM_{2.5}$ bias. Given that emissions levels of primary $PM_{2.5}$ and NO were the same for both models, these results in turn implied that a difference in transport was the cause of the model differences.

While both models make use of the same wind fields, the two models differ significantly in their approach to vertical diffusion. As noted above, AURAMS makes use of a Laasonen implicit approach to solve the equations for vertical diffusion, while CMAQ uses Crank–Nicolson (cf. Richtmyer, 1994). AURAMS also includes a Crank–Nicolson algorithm option – its use did not reduce AURAMS' $PM_{2.5}$ positive bias. The diffusion coefficients used by the models also differ: AURAMS makes use of the diffusion coefficients provided by the driving meteorological model GEM, then truncates their values with a lower limit of $0.1\,m^2\,s^{-1}$. CMAQ recalculates diffusion coefficients internally using other fields from the driving meteorology, but then truncates their values with a lower limit of $1.0\,m^2\,s^{-1}$. The diffusion coefficients generated by the CMAQ algorithm prior to the lower limit truncation were found to produce values similar in magnitude to the GEM weather forecast model's values in other work (Kelly et al., 2012). The main remaining difference between the two base models was thus the magnitude of the assumed lower limit for the diffusion coefficients.

An AURAMS sensitivity test was conducted to determine the impact of the magnitude of the cut-off in diffusion coefficient values on the model results, with $1.0\,m^2\,s^{-1}$ being used in AURAMS, for one selected day during the study period. The results of this test were dramatic and are shown in Fig. 3. The use of the higher diffusion coefficient





GMDD
6, 5595–5644, 2013

cut-off halved the AURAMS $NO_x$ and $PM_{2.5}$ maxima, and resulted in higher night-time $O_3$ levels: the test confirmed that the main cause of the differences between the models was the use of a higher value for the minimum diffusion coefficient in CMAQ.

The use of a higher level of diffusion than predicted by meteorological models is intended to compensate for these models' inability to resolve turbulence at smaller scales, particularly in urban regions. Recent work suggests that although improvements to turbulence parameterizations may result in some improvements in model $PM_{2.5}$ performance, a cut-off is still necessary to optimize $PM_{2.5}$ results (Pleim and Gilliam, 2012). Our above analysis suggests that in the use of a lower-limit cutoff for the model diffusion coefficients often results in degraded and unrealistic ozone performance at night, and may influence positive biases in the ozone concentration on the following day. The use of a relatively high cut-off for the diffusion coefficients allows greater vertical mixing to occur at night, allowing the emitted NO to be distributed over a larger vertical volume, reducing $O_3$ titration and allowing more $O_3$ to be mixed downwards into the lower part of the model. These effects allow the morning ozone production on the subsequent day to start from a higher level than would otherwise be the case, which may in turn allow $O_3$ to reach higher levels by the late afternoon. While this change in initial morning $O_3$ levels may contribute to the difference in the model results for $O_3$, it should be noted that this is not always the most significant factor, in that Fig. 2a shows that AURAMS and CMAQ sometimes have similar daytime $O_3$ peak levels despite having very different $O_3$ morning minima.

Given the difficulty in achieving good performance for both $O_3$ and $PM_{2.5}$ via the use of a larger cut-off in diffusion coefficients, our focus for most of our subsequent analysis became the emissions. Most of the nightime $PM_{2.5}$ predicted by the model was primary in origin (i.e. directly emitted), hence potential errors in emissions magnitude, timing, or spatial distribution may also play a critical role in setting night-time $PM_{2.5}$ concentrations. Consequently, we examine below the emissions for our domain in some detail, and conduct several tests to determine the impact of improvements to the emissions





GMDD
6, 5595–5644, 2013

and of model sensitivity to emissions changes, in addition to the use of a lower limit in diffusion coefficient values.

### 4.2 Scenarios

The above work led to three levels of analysis and revisions to the emissions, with a focus on the Canadian emissions data with which the authors have the greatest familiarity. The first level ("Emissions 1") identified the top 20 emitting sources for $PM_{2.5}$ and NO on the Canadian side of the domain. The temporal and spatial surrogate assignments for these sources were reviewed in detail to identify possible sources of $PM_{2.5}$ positive biases (the sensitivity to the annual totals in the emissions inventories were not directly examined here). This identified errors in both spatial and temporal fields, described below, which were consequently corrected. The second level ("Emissions 2") repeated the above analysis, but for the top 50 emitters in the four grid-squares comprising the urban core of the city of Vancouver. The reasoning underlying this second analysis was that many large sources of $PM_{2.5}$ occur outside the urban core, hence the analysis of Emissions 1 may miss spatial and temporal allocation errors important for the urban regions where the errors have the greatest impact on the model positive biases. The third level ("Emissions 3") was to examine the impact of improving stack parameter information for primary $PM_{2.5}$ emissions, for the specific sources in the four urban Vancouver grid-squares. The details of these three stages of analysis are described below.

#### 4.2.1 First level emissions analysis: totals on the Canadian portion of the grid

Upon examining the top 20 annual sources of Canadian emissions, several deficiencies in temporal and spatial allocation were identified.

*Temporal allocation:* The links to these sources' monthly, weekly and diurnal temporal allocation fields were used to construct grid-total time series of emissions of $PM_{2.5}$ and NO for the summer period simulated here, allowing the relative importance of the different sources on the Canadian side of the domain during the day to be determined. The temporal profiles for on-road mobile emissions were updated based on new measurement data (Zhang et al., 2011). The temporal profiles of 21 other activities were found to be inappropriate upon review. For example, charcoal grilling (residential and commercial) was assumed to have a "flat" profile, unchanging with month, day of week, or hour, despite the seasonality of the residential portion of this activity, and the absence of this activity in late night and early morning hours. This source was the second to 4th largest source of primary $PM_{2.5}$ at night, due to this flat profile. "Wood stoves and furnace boilers", and "fireplaces" were found to have a time-independent monthly profile (despite reduced heating energy needs in the summer, the time of the simulations of interest). Several activities (e.g. fertilizer application, land-spreading of manure, agricultural tractors, agriculture production) made use of simple sinusoidal diurnal temporal profiles offset from zero – hence late-night and early morning emissions of these daytime activities were non-zero. The temporal profile for fugitive dust emissions from paved and unpaved roads did not follow the known activity levels associated with mobile emissions (and the profile used for the former resulted in higher night-time emissions levels than that used for the latter). Marine vessel emissions were assumed to follow the temporal profile for railways. These inappropriate temporal allocation links were corrected:

1. The diurnal profile for charcoal grilling was revised to take commercial and residential activity levels into account, with zero emissions late at night and in the early morning hours.

2. The monthly profile for woodstoves/furnace boilers and for fireplaces were modified to take seasonal energy use into account.

3. The agricultural temporal profile was modified from an sinusoid with trough value greater than zero to a sinusoid which reached zero levels in the late evening/early morning.





GMDD
6, 5595–5644, 2013

4. Fugitive dust emissions from paved and unpaved roads were assumed to follow the same diurnal profile as mobile emissions activities.

5. Marine vessels were assumed to have a constant diurnal profile (this was a relatively minor change; the railway profile used earlier having been almost constant as well).

*Spatial allocation:* Six new spatial surrogates were generated for mobile emissions (Zhang et al., 2011). Four activities associated with the mining industry were found to be linked to spatial surrogates that had maxima in urban regions – these linkages were switched to an existing "total mining" surrogate which better reflected the location of actual mining activities in the domain (the original surrogate included mining head offices as "mining activities", resulting in emissions being allocated in urban Vancouver instead of the actual mining locations, see Fig. 4). Twenty-five spatial surrogates were improved through the incorporation of new GIS fields for the Lower Fraser Valley.

#### 4.2.2 Second level emissions analysis, Vancouver urban grid squares

*Temporal allocation:* in a manner similar to the first level analysis, a list of the top 50 annual emitters corresponding to four downtown Vancouver grid-cells was generated. These were linked to monthly, weekly and diurnal temporal profiles, and the resulting time series examined for accuracy with respect to the emitting activities. The resulting total emission time series for the nine largest of these sources is shown in Fig. 5. Four activities were found to be linked to profiles with no or minimal expected diurnal variation. Emissions from "other industry" were assumed to be time-invariant, despite the diurnal nature of most human activities. Asphalt paving and roofing was assumed to take place on an almost time-invariant diurnal profile (the same as used for railway emissions). "Concrete/gypsum/plaster products" and "bulk materials storage; all storage types; cement" were assumed to make use of the sinusoidal profile offset from zero mentioned above. All four of these sources were linked to a new diurnal profile which zeroed emissions during the night between 22:00 and 05:00 LT.





GMDD
6, 5595–5644, 2013

*Spatial allocation*: two spatial allocation fields, "coal industry – coal cleaning" and "mining industry crawler/tractors" were found to have maxima in urban regions – a revised linkage to the new total mining surrogate was used to take into account the actual location of mining industries.

#### 4.2.3 Third level of emissions investigation, specific point sources

For one of the grid-squares in urban Vancouver, minor point sources dominate as a group for $PM_{2.5}$ emissions, compared to major point, non-mobile area sources, and mobile area sources. Only the operators of point sources with stack heights greater than or equal to 50 m altitude are required under Canadian legislation to report stack parameters (height, diameter, exit temperature, exit velocity) associated with emissions to the Canadian National Pollutant Release Inventory (NPRI). Consequently, all stacks with elevations less than 50 m are treated as surface area sources within the Canadian portion of the domain, and the absence of plume rise in the subsequent vertical distribution of emissions may result in surface-level over-predictions of particulate matter. Point sources in the USA are available at lower heights, but a cut-off of 30 m is usually used to reduce the number of sources for which plume rise calculations are required. Municipal-level reporting of stack parameters is, however, required for all sources in the Metro Vancouver jurisdiction. For the four largest of these facilities, the original $PM_{2.5}$ emissions totals (NPRI, treated as area sources) were replaced with Metro Vancouver data that included stack parameters, allowing vertical redistribution of emissions to take place, as a sensitivity test on the predicted local $PM_{2.5}$ levels.

#### 4.2.4 Non-mobile area source primary PM emissions sensitivity simulations

A further analysis of $PM_{2.5}$ emissions subsequent to the above changes examined urban diurnal profiles on the basis of four main emissions categories; major point sources, minor point sources, mobile area sources and non-mobile area sources. Non-mobile area sources dominated primary $PM_{2.5}$ emissions (particularly in US cities





GMDD
6, 5595–5644, 2013

where the above Canadian emissions changes were not applied). While some of the largest of these sources were considered in the above analysis (on the Canadian side of the grid), many smaller magnitude area sources also contributed to total emissions. Diurnal profiles of total area source emissions from the processed emissions data typically showed an offset sinusoidal shape (i.e. a temporal profile with a positive offset diurnal sinusoidal variation contributed to the bulk of the non-mobile area source emissions). In order to examine the relative important of the diurnal variation in emissions from these sources at night, a final test simulation was carried out. The original emissions of all non-mobile area sources were modified using a smoothed square-wave function which reduced the emissions during the night and increased them during the day, preserving the total mass of emissions, yet emitting proportionately less at night and more during the day. Figure 6 compares the time series of grid total emissions of PM from these sources before and after this change. Note that we do not justify this final sensitivity simulation on the basis of observations of the diurnal behaviour of the myriad of sources comprising the non-mobile emissions sector. Rather, the intent of the simulation is to show the extent to which that diurnal emissions behaviour of non-mobile area source may impact the resulting concentration predictions. This in turn highlights the relative importance of accurate temporal allocation information towards the model accuracy.

#### 4.2.5 Upgrades to AURAMS

Ongoing improvements to AURAMS during the course of this study included changing from the AURAMS default operator splitting setup (one-step forward operator splitting) to centered operator splitting, eliminating an additional source of differences between CMAQ and AURAMS. This was found to have a significant impact on sea-salt aerosol production, significantly reducing levels offshore. In addition, the particle dry deposition algorithm was upgraded to treat particle settling and deposition in a semi-Lagrangian approach, and conservation of column mass was enforced in the vertical diffusion algorithm through separation of the area emissions, diffusion and gaseous deposition into three different operators. A separate test of this suite of changes was conducted in order to determine their impact on model performance (AURAMS1b in the subsequent discussion).

### 4.3 Quantitative comparison of the impacts of the changes to the model and emissions

The above analysis led to seven model simulations in addition to the original base case. These scenarios are outlined in Table 2, with statistical results in Tables 4 and 5.

The hourly $O_3$ and $PM_{2.5}$ predictions from the above simulations were compared to observations as described above; summary tables of the statistical results for the entire grid are shown in Table 4a ($O_3$) and b ($PM_{2.5}$). The 2nd column of the table shows observed mean, maximum and minimum values. The third and fourth columns show the results of the initial base case comparison with observations, with normal font showing the model with the lower score, and bold font showing the model with the higher score. In the subsequent columns, the model results are compared to their respective base case simulation. Normal font indicates unchanged performance, normal italics indicates worse performance relative to the base case, and bold italics indicates better performance than the base case. Figures 7 and 8 show binned scatterplots of the model simulations of $O_3$ and $PM_{2.5}$ vs. observations for the runs analyzed in Table 4a and b.

#### 4.3.1 Impact of AURAMS code improvements

The improvements to AURAMS' code improved statistical scores for all $O_3$ measures (Table 4b) except for the maximum and minimum $O_3$, which saw a slight decrease. Comparison of Fig. 7b and d show a relatively minor impact on the overall scatter between observations and model values for these changes, with a more pronounced difference visible between the two models (e.g. Fig. 7a vs. b). Conversely, $PM_{2.5}$ scores became worse with the exception of maximum $PM_{2.5}$ and the slope: Fig. 8b and d suggest a slight increase in $PM_{2.5}$ values. Despite the statistical differences noted, the impact of the model improvements on the visual appearance of the scatterplots was minor.

#### 4.3.2 Impact of first level emissions improvements

For CMAQ, the improvements to the emissions had a mixed effect on the model results. Ozone scores for the mean, mean bias, mean absolute error, mean squared error, root mean square error, normalized mean bias and normalized mean error all improved relative to the base case, while performance was degraded for maximum, minimum, *y* intercept, slope, and correlation coefficient. Figure 7a and c show the lower slope and increased *y* intercept noted in the table. CMAQ tended to underpredict the maximum $O_3$ values (lower values on the *y* axis Fig. 7c compared to 7a). All CMAQ $PM_{2.5}$ scores were degraded with the use of the improved emissions, with the exception of the *y* intercept. Comparing Fig. 8a and c suggests that one impact of the stage 1 emissions change was to decrease CMAQ's ability to simulate $PM_{2.5}$ maxima, which is reflected in the statistics. For AURAMS, the use of the first level of emissions improvements resulted in improvements for all $O_3$ statistics except maximum and minimum. Figures 7d and e are broadly similar: the improvements to AURAMS' $O_3$ predictions do not result in a substantially different scatter distribution. The statistical measures for AURAMS' $PM_{2.5}$ with the stage 1 emissions improved relative to the base case with the exception of the minimum, mean absolute error, and normalized mean error, all of which showed a slight degradation of performance. Differences in $PM_{2.5}$ scatter for the stage 1 emissions are minor: a slight shift of the distribution to the right (compare Fig. 8b, d and e. Comparing the columns in Table 4a for AURAMS simulations to isolate the impact of the emissions improvements alone on that model, it can be seen that the $O_3$ scores for slope and correlation coefficient have improved, while the other scores have degraded, while for $PM_{2.5}$ all statistics with the exception of the minimum $PM_{2.5}$ have improved.

The relative success of the first level of improved emissions data thus appears to be species and model dependant. The revised emissions had a mixed impact on CMAQ's





GMDD
6, 5595–5644, 2013

$O_3$ performance, and degraded CMAQ's $PM_{2.5}$ performance over most statistics. For AURAMS (considering the impact of emissions alone), $O_3$ performance was degraded slightly, while $PM_{2.5}$ performance generally improved.

#### 4.3.3 Impact of second and third level emissions improvements

The second level of emissions improvements (applied only to AURAMS; "AURAMS3" columns of Table 4a and b) results in further improvements to most $O_3$ statistics, though a reduction in performance for $PM_{2.5}$ for statistics other than maximum, slope and correlation coefficient. The differences relative to the first level of emissions changes are difficult to distinguish visually Figs. 7 and 8e and f.

The third level of emissions improvements (applied only to AURAMS; "AURAMS4") showed no impact on $O_3$ (as expected, since the final level of improvements was a sensitivity test applied only to primary $PM_{2.5}$ emissions, hence Fig. 7f and g are identical). Changes to the $PM_{2.5}$ statistics across the grid were relatively minor due to this test (as might be expected given that the emissions were modified in only 4 grid squares in urban Vancouver). However, differences in the outer envelope of the corresponding scatterplot (Fig. 8f and g) can be observed: the third level emissions scenario changes the distribution for cases of high model over-prediction.

#### 4.3.4 Impact of a diffusivity cutoff

The application of a diffusion cut-off of $0.6\,m^2\,s^{-1}$ ("AURAMS5") resulted in a degradation of AURAMS' $O_3$ performance for all scores except for correlation coefficient, while improving AURAMS's $PM_{2.5}$ performance for all scores except for maximum, minimum, slope and correlation coefficient. The scatterplots for this simulation, Figs. 7 and 8h, are significantly different from the other scatterplots for AURAMS. For $O_3$ (Fig. 7h), more of the points are clustered in the center of the distribution, reflecting the improvement in statistics such as the RMSE. However, there are also many points along the *y* axis which are now in the hotter colours in Fig. 7h, indicating instances where





GMDD
6, 5595–5644, 2013

the observed $O_3$ was close to zero, while the modelled $O_3$ was sometimes as high as 30 ppbv. These points correspond to cases of night-time underprediction of NO titration of $O_3$, described earlier. The scatter for $PM_{2.5}$ improved significantly, with the removal of many of the high values, and a better distribution about the 1 to 1 line than any of the other simulations. As before, $PM_{2.5}$ improvements via this approach came with the cost of $O_3$ performance degradation.

#### 4.3.5 Impact of temporal renormalization of non-mobile area sources

Renormalizing the non-mobile area sources ("AURAMS6") so that less emissions of all species occur at night ("AURAMS6") improved $O_3$ performance for all scores except the minimum and slope (correlation coefficient was unchanged), while *also* improving all scores for $PM_{2.5}$ aside from the minimum and the slope (which was unchanged). The corresponding scatterplots (Figs. 7 and 8i) show some of the same behaviour as the previous run ("AURAMS5", Figs. 7h and 8h); the number of $O_3$ points close to the 1 to 1 line have increased relative to other simulations, and the number of $PM_{2.5}$ points with very high over-predictions has decreased and the distribution about the 1 to 1 line has improved, though not to the same extent as diffusion cut-off simulation.

The final two simulations are compared relative to the base case AURAMS1 simulation in Fig. 9. One impact of using a higher diffusion cut-off for $O_3$ (Fig. 9a) is an increase in the number of counts close to the *y* axis (i.e. $O_3$ minima are increasing), while the temporal redistribution of emissions (Fig. 9b) results in both increases and decreases in low level $O_3$ predictions. The higher diffusion cut-off causes $PM_{2.5}$ to trend downward relative to the base case (Fig. 9c), while the redistribution of emissions has a more uniform distribution across the 1 to 1 line, with slightly greater counts below the line (Fig. 9d).

#### 4.3.6 Model performance in the Lower Fraser Valley

The performance of the models for $PM_{2.5}$ across the five Lower Fraser Valley stations is shown in Table 5. Here, the base case performance of the two models is mixed, with each model outscoring the other for 7 out of 14 statistical measures. The first level of emissions upgrades has degraded CMAQ's performance as before. The introduction of the $0.6\,m^2\,s^{-1}$ diffusion cut-off and the renormalizing of non-mobile area source emissions have a similar impact on improving model results, while the diffusion cut-off degrades $O_3$ performance for all measures except maximum and correlation coefficient (not shown).

Example model time series for $O_3$ and $PM_{2.5}$ are compared to observations in Figs. 10 through 12. The degradation in CMAQ $O_3$ performance with the use of the first level of emissions upgrades is noticeable as increases in night-time $O_3$ levels (e.g. compare Fig. 2, minima on the night of 30 July). AURAMS' $O_3$ maxima increase with the use of the first level emissions change, while AURAMS' $PM_{2.5}$ levels decrease, sometimes substantially (cf. night of 26 July, Fig. 10b). The subsequent levels of emissions changes have relatively little impact on $O_3$ (Fig. 11a), though local reductions in $PM_{2.5}$ continue (Fig. 11b). Figure 12 shows the local impact of a cut-off in diffusion of $0.6\,m^2\,s^{-1}$ to that of a reduction in non-mobile area source emissions at night. In both cases, night-time $O_3$ levels are erroneously increased, and night-time $PM_{2.5}$ levels are decreased.

## 5 Discussion

The work described above suggests the following:

1. The choice of a larger magnitude for a minimum cut-off in diffusivity may sometimes lead to insufficient titration of ozone at night, and/or mixing of higher level ozone downwards, creating erroneously high $O_3$ predictions at night and potentially resulting in higher $O_3$ predictions during the day. When a higher cut-off in





GMDD
6, 5595–5644, 2013

diffusivity was tested within AURAMS, $PM_{2.5}$ scores were improved, but at the expense of degrading $O_3$ scores, particularly at night. If model $PM_{2.5}$ emissions are erroneously high, the use of a high diffusivity cut-off may compensate for these errors, lowering $PM_{2.5}$. This suggests that hourly ozone performance should be used as another means of ensuring that compensating errors of this nature are not taking place.

2. The hypothesis that at least some of the $PM_{2.5}$ prediction errors may result from errors in the emissions inputs has some merit. A series of tests to model emissions in which temporal and spatial allocation errors were corrected, and changes in diurnal profiles were investigated, showed a similar improvement to a diffusion cut-off approach, without degrading $O_3$ performance or even causing it to improve. This indicates that model performance is at least as sensitive to the level of accuracy of the magnitude and spatial and temporal allocation of the driving emissions data as to the parameterization of vertical mixing. Further, the practice of choosing a minimum diffusion level to balance ozone vs. $PM_{2.5}$ errors (CMAS, 2006) is of limited value – further improvements to the accuracy of the $PM_{2.5}$ are achievable through the collection of improved area-source temporal and spatial emissions data.

3. There may also be other factors which may act to reduce "effective" $PM_{2.5}$ emissions. For example, fugitive emissions of $PM_{2.5}$ are subject to land-use-dependant reduction factors to account for the very local-scale uptake of $PM_{2.5}$ to vegetation, sometimes resulting in significant reductions from the inventory emissions levels for fugitive sources (c f. Pace, 2005). Similar local reduction/local availability factors may be worth considering for other $PM_{2.5}$ sources.

4. We note that the accuracy of the relative magnitude of the emissions of different species is also important. For example, if the $NO_x$ emissions alone are currently underestimated, then the negative impact of a higher level for the cut-off in minimum diffusion on $O_3$ performance would be decreased.

5. At least some of AURAMS $PM_{2.5}$ over-predictions may still reside in vertical mixing issues: model values were still biased positive over all emissions improvement and sensitivity runs performed here, indicating that other processes are required to reduce $PM_{2.5}$ levels.

6. It should be noted that the current work is limited in that only emissions and diffusivity approaches were examined in detail as a cause for differences between the two model results. The model errors in general may also be reduced through adopting a higher resolution, to better simulate the complex topography in the region. For example, the models make use of different deposition parameterizations, and Nopmongcol et al. (2012) found that models with relatively high deposition rates for $PM_{2.5}$ were biased low for their overall performance. While changes to the timing of primary emissions of $PM_{2.5}$ were shown to potentially account for much of the differences between the two models, changes to the particle deposition velocity algorithms may account for the remaining positive bias in AURAMS, and negative bias in CMAQ, for $PM_{2.5}$. This should be examined in future work Also, while we have focussed on the Lower Fraser Valley in some of our analyses, the relative importance of the different processes may differ in other parts of the model domain.

7. Our work has focussed on the differences between the two models, but has important implications for the broader issue of explaining the causes for the formation of $O_3$ and $PM_{2.5}$ in urban and downwind environments. Our results suggest that discrepancies between simulated and observed night-time chemistry can not be explained via increases in turbulence alone. We have identified the timing and placement of primary $PM_{2.5}$ emissions from area sources as a key factor in explaining the magnitude and timing of observed $PM_{2.5}$ concentrations.





GMDD
6, 5595–5644, 2013

## 6 Conclusions

The CMAQ and AURAMS models were compared, using a common horizontal map projection and grid spacing, a common set of meteorological inputs, and a common emissions inventory and emissions processing system, for a domain on the north-western coast of North America, for a 1 month simulation for the summer of 2005. The initial model results were markedly different, with AURAMS having significantly better performance for $O_3$ than CMAQ, while CMAQ's performance for $PM_{2.5}$ was better than that of AURAMS. One of the main factors leading to the differences was found to be the magnitude of the assumed lower limit in the coefficient of vertical diffusion employed in each model, with the adoption of a higher value in AURAMS resulting in performance more like that of CMAQ. Improvements in $PM_{2.5}$ performance associated with the lower cut-off were also associated in degraded performance for $O_3$. A subsequent investigation of local emissions through improvements to spatial and temporal allocations and sensitivity tests showed that $PM_{2.5}$ performance could be improved through emissions improvements, without degrading $O_3$ performance. The model results were shown to have a similar level of sensitivity to emissions spatial and temporal allocation as to lower limits on vertical mixing.

The findings have important implications for our understanding of $O_3$ and $PM_{2.5}$ in urban environments, in that they demonstrate that increases in turbulent mixing are insufficient to explain the discrepancies between observations and simulations for these species. Further, assuming increased levels of turbulence may mask the relative importance of other factors in setting concentration levels, particularly at night. Here, we have found that the heretofore inadequately resolved timing and spatial allocation of $PM_{2.5}$ primary emissions, specifically from the area source sector, may have a considerable influence on $PM_{2.5}$ concentrations. We therefore recommend improvements to area-source primary $PM_{2.5}$ emissions data as a focus for future measurement and modelling work.





GMDD
6, 5595–5644, 2013

These results should not be taken to imply that increases in turbulent diffusivity and/or other factors should be ruled out as a line of investigation for achieving improved model performance. Both emissions (timing, spatial distribution, and magnitude) and the magnitude of turbulent diffusion were shown to be of potential importance here. Our results suggest that both processes are complementary routes for further model improvements. However, model performance for both $O_3$ and $PM_{2.5}$ should be simultaneously evaluated in future work, to ensure that improvements in one predicted species are not offset by degraded model performance in the other.

## References

Ainslie, B., Steyn, D. G., Reuten, C., and Jackson, P. L.: A retrospective analysis of ozone formation in the Lower Fraser Valley, British Columbia, Canada, Part 2: influence of emissions reductions on ozone formation, Atmosphere-Ocean, 51, 2, 170–186, 2013.

Brook J. R., Strawbridge, K., Snyder, B. J., Boudries, H., Worsnop, D., Anlauf, K., Sharma, S., Lu, G., and Hayden, K.: Towards an understanding of the fine particle variations in the LFV: integration of chemical, physical and meteorological observations, Atmos. Environ., 38, 5775–5788, 2004.

Carr, D., Lewin-Koh, N., and Maechler, M.: hexbin: Hexagonal Binning Routines. R package version 1.24.0, available at: http://CRAN.R-project.org/package=hexbin (last access: 17 October 2013), 2010.

Carslaw, D. and Ropkins, K.: openair: Open-source tools for the analysis of air pollution data, R package version 0.4-15, 2011.

Carter, W. P. L.: Documentation of the SAPRC-99 Chemical Mechanism for VOC Reactivity Assessment, Final Report to California Air Resources Board Contract 92–329 and Contract 95–308, Available at: http://www.engr.ucr.edu/~carter/reactdat.htm (last access: 17 October 2013), 2000a.

Carter, W. P. L.: Implementation of the SAPRC-99 Chemical Mechanism into the Models-3 Framework. Report to the United States Environmental Protection Agency, available at: http://pah.cert.ucr.edu/~carter/reactdat.htm (last access: 17 October 2013), 2000b.





GMDD
6, 5595–5644, 2013

CEP: Carolina Environmental Program, Sparse Matrix Operator Kernel Emission (SMOKE) modelling system, University of North Carolina, Carolina Environmental Programs, Chapel Hill, NC, see http://www.smoke-model.org/index.cfm (last access: 17 October 2013), 2003.
Côté, J., Gravel, S., Méthot, A., Patoine, A., Roch, M., and Staniforth, A.: The operational CMC-MRB Global Environmental Multiscale (GEM) model, Part 1: Design considerations and formulation, Mon. Weather Rev., 126, 1373–1395, 1998.
CMAS: available at: http://www.cmascenter.org/cmaq/documentation/4.6/ADVECTION_DIFFUSION.txt (last access: 19 September 2013), 2006.
Deepayan, S.: Lattice: Multivariate Data Visualization with R, Springer, New York, ISBN 978-0-387-75968-5, 2010.
Galmarini, S. and Rao, S. T.: The AQMEII two-continent regional air quality model evaluation study: fueling ideas with unprecedented data, Atmos. Environ., 45, p. 2464, 2011.
Gong, W., Dastoor, A. P., Bouchet, V. S., Gong, S., Makar, P. A., Moran, M. D., Pabla, B., Menard, S., Crevier, L.-P., Cousineau, S., and Venkatesh, S.: Cloud processing of gases and aerosols in a regional air quality model (AURAMS), Atmos. Res., 82, 248–275, 2006.
Houyoux, M. R., Vukovich, J. M., Coats Jr., C. J., and Wheeler, N. J. M.: Emission inventory development and processing for the Seasonal Model for Regional Air Quality (SMRAQ) project, J. Geophys. Res., 105, 9079–9090, 2000.
Kelly, J., Makar, P. A., and Plummer, D. A.: Projections of mid-century summer air-quality for North America: effects of changes in climate and precursor emissions, Atmos. Chem. Phys., 12, 5367–5390, doi:10.5194/acp-12-5367-2012, 2012.
Makar, P. A., Gong, W., Mooney, C., Zhang, J., Davignon, D., Samaali, M., Moran, M. D., He, H., Tarasick, D. W., Sills, D., and Chen, J.: Dynamic adjustment of climatological ozone boundary conditions for air-quality forecasts, Atmos. Chem. Phys., 10, 8997–9015, doi:10.5194/acp-10-8997-2010, 2010.
McKeen, S., Wilczak, J., Grell, G., Djalalova, I., Peckham, S., Hsie, E.-Y., Gong, W., Bouchet, V., Menard, S., Moffet, R., McHenry, J., McQueen, J., Tang, Y., Carmichael, G. R., Pagowski, M., Chan, A., Dye, T., Frost, G., Lee, P., and Mathur, R.: Assessment of an ensemble of seven real-time ozone forecasts over eastern North America during the summer of 2004, J. Geophys. Res., 110, D21307. doi:10.1029/2005JD005858, 2005.
McKeen, S., Chung, S. H., Wilczak, J., Grell, G., Djalalova, I., Peckham, S., Gong, W., Bouchet, V., Moffet, R., McHenry, J., Tang, Y., Carmichael, G. R., Mathur, R., and Yu, S.:

Evaluation of several $PM_{2.5}$ forecasts using data collected during the ICARTT/NEAQS 2004 field study, J. Geophys. Res., 112, D10S20, doi:10.1029/2006JD007608, 2007.

McKeen, S., Grell, G., Peckham, S., Wilczak, J., Djalalova, I., Hsie, E.-Y., Frost, G., Peischl, J., Schwarz, J., Spackman, R., Holloway, J., de Gouw, J., Warneke, C., Gong, W., Bouchet, V., Gaudreault, S., Racine, J., McHenry, J., McQueen, J., Lee, P., Tang, Y., Carmichael, G. R., and Mathur, R.: An evaluation of real-time air quality forecasts and their urban emissions over eastern Texas during the summer of 2006 Second Texas Air Quality Study field study, J. Geophys. Res., 114, D00F11, doi:10.1029/2008JD011697, 2009.

Nopmongcol, U., Koo, B., Tai, E., Jung, J., Piyachaturawat, P., and Sportisse, B.: Modeling Europe with CAMx for the air quality model evaluation international initiative (AQMEII), Atmos. Environ., 53, 60–74, 2012.

Pace, T. G.: Methodology to estimate the transportable fraction (TF) of fugitive dust emissions for regional and urban scale air quality analyses (8/3/2005 Revision), Internal report, US EPA, Research Triangle Park, North Carolina, 12 pp, available at: http://www.epa.gov/ttn/chief/emch/dustfractions/transportable_fraction_080305_rev.pdf (last access: 17 October 2013), 2005.

Pierce, D.: ncdf: Interface to Unidata netCDF data files, R package version 1.6.3, available at: http://CRAN.R-project.org/package=ncdf (last access: 17 October 2013), 2010.

Pleim, J. E.: A combined local and nonlocal closure model for the atmospheric boundary layer, Part 1: Model description and testing, J. Appl. Meteorol. Climatol., 46, 1383–1395, 2007a.

Pleim, J. E.: A combined local and nonlocal closure model for the atmospheric boundary layer, Part 2: Application and evaluation in a mesoscale meteorological model, J. Appl. Meteorol.and Climatology, 46, 1396–1409, 2007b.

Pleim, J. E. and Gilliam, R: Simple urban parameterization for WRF-CMAQ, 2012 CMAS conference, available at: https://www.cmascenter.org/conference/2012/slides/pleim_simple_urban_2012.pptx (last access: 17 October 2013), 2012.

Pleim, J. E., Roselle, S. J., Bhave, P. V., Bullock, O. R., Hutzell, W. T., Luecken, D. J., Nolte, C. G., Sarwar, G., Schere, K. L., Young, J., Godowitch, J., and Appel, K. W.: The 2006 CMAQ Release and Plans for 2007, Extended abstract for the 5th CMAS Conference, Chapel Hill, NC, 16–18 October 2006, available at: http://www.cmascenter.org/conference/2006/agenda.cfm (last access: 17 October 2013), 2006.





GMDD
6, 5595–5644, 2013
Transport, emissions, & compensating errors in chemical models
P. A. Makar et al.

R Development Core Team: R: A language and environment for statistical computing. R Foundation for Statistical Computing, Vienna, Austria, ISBN 3-900051-07-0, available at: http://www.R-project.org (last access: 17 October 2013), 2010.

Richtmyer, R. D.: Difference methods for initial value problems, Krieger Pub. Co., Malabar, Fla., 405 pp., 1994.

Smyth, S. C., Jiang, W., Yin, D., Roth, H., and Giroux, E.: Evaluation of CMAQ $O_3$ and $PM_{2.5}$ performance using Pacific 2001 measurement data, Atmos. Environ., 40, 2735–2749, 2006.

Smyth, S. C., Jiang, W., Roth, H., Moran, M. D., Makar, P. A., Yang, F., Bouchet, V. S., and Landry, H.: A comparative performance evaluation of the AURAMS and CMAQ air-quality modelling systems, Atmos. Environ., 43, 1059–1070, 2009.

Solazzo, E., Bianconi, R., Vautard, R., Appel, K. W., Moran, M. D., Hogrefe, C., Bessagnet, B., Brandt, J., Christensen, J. H., Chemel, C., Coll, I., van der Gon, H. D., Ferriera, J., Forkel, R., Francis, X. V., Grell, G., Grossi, P., Hansen, A. B., Jericevic, A., Kraljevic, L, Miranda, A. I., Noppmongcol, U., Priovano, G., Prank, M., Riccio, A., Sartelet, N., Schaap, M., Silver, J. D., Sokhi, R. S., Vira., J., Werhahn, J., Wolke, R., Yarwood, G., Zhang, J., Rao, S. T., and Galmarini, S.: Model evaluation and ensemble modelling of surface-level ozone in Europe and North America in the context of AQMEII, Atmos. Environ., 53, 60–74, 2012a.

Solazzo, E., Bianconi, R., Priovano, G., Matthias, V., Vaurtard, R., Moran, M. D., Appel, K. W., Bessagnet, B., Brandt, J., Christensen, J. H., Chemel, C., Coll, I., Ferreira, J., Forkel, R., Francis, X. V., Grell, G., Grossi, P., Hansen, A. B., Miranda, A. I., Nopmoncol, U., Prank, M., Sartelet, K. N., Schaap, M., Silver, J. D., Sokhi, R. S., Vira, J., Werhahn, J., Wolke, R., Yarwood, G., Zhnag, J., Rao, S. T., and Galmarini, S.: Operational model evaluation for particulate matter in Europe and North America in the context of AQMEII, Atmos. Environ., 53, 75–92, 2012b.

Steyn, D. G., Ainslie, B., Reuten, C., and Jackson, P. L.: A retrospective analysis of ozone formation in the Lower Fraser Valley, British Columbia, Canada, Part 1: Dynamical model evaluation, Atmos.-Ocean, 51, 153–169, doi:10.1080/07055900.2013.781940, 2013.

Stockwell, W. R. and Lurmann, F. W.: Intercomparison of the ADOM and RADM Gas-Phase Chemical Mechanisms, Electrical Power Research Institute Topical Report, EPRI, 3412 Hillview Avenue, Palo Alto, CA, 254 pp., 1989.

Xiu, A. and Pleim, J. E.: Development of a land surface model, Part 1: Application in a mesoscale meteorology model. J. Appl. Meteorol., 40, 192–209, 2000.

Zhang, J., Zheng, Q., Moran, M. D., Gordon, M., Liggio, J., Makar, P., Stroud, C., and Taylor, B.: Improvements to SMOKE Processing of Canadian On-Road Mobile Emissions, 2012 International Emission Inventory Conference, Tampa, Florida – 13–16 August 2012, available at: http://www.epa.gov/ttn/chief/conference/ei20/session1/jzhang.pdf (last access: 17 October 2013), 2011.

Zhang, L., Gong, S.-L., Padro, J., and Barrie, L.: A size-segregated particle dry deposition scheme for an atmospheric aerosol module, Atmos. Environ., 35, 549–560, 2001.

Zhang, L., Moran, M. D., Makar, P. A., Brook, J. R., and Gong, S.-L.: Modelling gaseous dry deposition in AURAMS – a unified regional air-quality modelling system, Atmos. Environ., 36, 537–560, 2002.

**Table 1.** Comparison of main features for the CMAQ and AURAMS models.

| | | |
|---|---|---|
| Model<br>Version | AURAMS<br>1.4.2 | CMAQ<br>4.6 |
| Horizontal Projection | Polar stereographic true at 60° N, 93 × 93 gridpoints; 12 km grid spacing | |
| Emissions Inventory | Anthropogenics: 2006 Canadian; 2005 US; processed using the Sparse Matrix Operating Kernel Emissions processing system. Biogenics: BEIS3.0.9, processed using model-predicted temperatures and PAR values. | |
| Particle Size Distribution | Sectional approach, 12 size bins | Modal Approach, 3 modes |
| Vertical Diffusion | Laasonen numerics, diffusion coefficients from GEM, internal eddy diffusivity minimum of 0.1 $m^2 s^{-1}$. | Internal calculation of eddy diffusivity, with internal minimum of 1.0 $m^2 s^{-1}$. |
| Number of Vertical Levels | 27 | 15 |
| Plume Rise | Calculated on-line | Pre-calculated in SMOKE |
| Dry Deposition | Gases: resistance parameterization based on Wesley (Zhang et al., 2002). Particles: (Zhang et al., 2001). | Modified RADM scheme with Pleim-Xiu land surface model (Xiu and Pleim, 2000). |
| Driving Meteorology | Global Environmental Multscale (GEM) model, version 3.2.2, overlapping 30 h simulations starting at 0Z, initial 6 h spin-up discared; final 24 h used for air-quality model input. | |
| Simulation Period | 15 Jul–15 Aug 2005 | |





GMDD
6, 5595–5644, 2013

**Table 2.** Description of model scenarios.

| Scenarios | Description |
|---|---|
| CMAQ1 | Base Case CMAQ |
| AURAMS1 | Base Case AURAMS |
| CMAQ2 | First level of emissions upgrades applied to CMAQ |
| AURAMS1b | AURAMS code improvements applied to AURAMS, no emissions changes |
| AURAMS2 | As in AURAMS 1b, with the first level of emissions upgrades |
| AURAMS3 | AURAMS 2 + second level of emissions upgrades |
| AURAMS4 | AURAMS 3 + third level of emissions upgrades |
| AURAMS5 | AURAMS4 + use of diffusion cut-off of 0.6 $m^2 s^{-1}$ |
| AURAMS6 | AURAMS5 + renormalization of non-mobile area source emissions. |





GMDD
6, 5595–5644, 2013



P. A. Makar et al.

**Table 3.** Statistical measures of model performance. $N$ is the number of paired observed-model values, $\overline{O}$ is the mean observed value, $\overline{M}$ is the mean model value.

| Statistical Measure | Description | Formula |
|---|---|---|
| R | Pearson Correlation Coefficient | $R = \frac{N\sum_{i=1}^{N}(O_i \cdot M_i) - \sum_{i=1}^{N}(M_i)\sum_{i=1}^{N}(O_i)}{\sqrt{N\sum_{i=1}^{N}(M_i \cdot M_i) - \sum_{i=1}^{N}(M_i)\cdot\sum_{i=1}^{N}(M_i)}\sqrt{N\sum_{i=1}^{N}(O_i \cdot O_i) - \sum_{i=1}^{N}(O_i)\cdot\sum_{i=1}^{N}(O_i)}}$ |
| a | Intercept of observations vs. model best-fit line | $a = \overline{M} - b \cdot \overline{O}$ |
| b | Slope of observations vs. model best-fit line | $b = \frac{\sum_{i=1}^{N}\left[\left(O_i - \overline{O}\right)\left(M_i - \overline{M}\right)\right]}{\sum_{i=1}^{N}\left[\left(O_i - \overline{O}\right)^2\right]}$ |
| MB | Mean bias | $\mathrm{MB} = \frac{1}{N}\sum_{i=1}^{N}(M_i - O_i)$ |
| MAE | Mean Absolute Error | $\mathrm{MAE} = \frac{1}{N}\sum_{i=1}^{N}\lvert M_i - O_i \rvert$ |
| MSE | Mean Square Error | $\mathrm{MSE} = \frac{1}{N}\sum_{i=1}^{N}(M_i - O_i)^2$ |
| RMSE | Root Mean Square Error | $\mathrm{RMSE} = \sqrt{\frac{1}{N}\sum_{i=1}^{N}(M_i - O_i)^2}$ |
| NMB | Normalized Mean Bias | $\mathrm{NMB} = \frac{\sum_{i=1}^{N}(M_i - O_i)}{\sum_{i=1}^{N} O_i} \times 100$ |
| NME | Normalized Mean Error | $\mathrm{NME} = \frac{\sum_{i=1}^{N}\lvert M_i - O_i \rvert}{\sum_{i=1}^{N} O_i} \times 100$ |





GMDD
6, 5595–5644, 2013

**Table 4.** (a) $O_3$ statistics, Entire Grid (ppbv). Third and fourth columns: Regular font/bold font corresponds to model with worse/better performance. Subsequent columns: regular font/italics/bold italics corresponds to unchanged/worse/better performance than the same model in original comparison.

| $O_3$ Statistics | OBS | CMAQ 1 Base Case | AURAMS 1 Base Case | CMAQ 2 Emissions 1 | AURAMS1b Code Improvements | AURAMS 2 Code Improvements + Emissions 1 | AURAMS 3 Code Improvements + Emissions 1, 2 | AURAMS 4 Code Improvements + Emissions 1, 2,3 | AURAMS 5 Diffusion Cut-off = 0.6 $m^2 s^{-1}$ | AURAMS 6 Renormalize Non-Mobile Area Sources |
|---|---|---|---|---|---|---|---|---|---|---|
| Number of Pairs | 41 846 | 41 789 | 41 846 | 41 846 | 41 846 | 41 846 | 41 846 | 41 846 | 41 846 | 41 846 |
| Mean | 22.67 | 39.79 | **31.16** | ***38.62*** | ***29.89*** | ***30.78*** | ***29.99*** | ***29.99*** | *33.05* | ***30.61*** |
| Maximum | 100 | 100.48 | **100.21** | *78.74* | *102.73* | *101.49* | *100.93* | *100.93* | *100.49* | ***99.87*** |
| Minimum | 0 | 1.26 | **3.7E-05** | ***0.36*** | *6.10E-05* | *5.20E-05* | *5.20E-05* | *5.20E-05* | *0.00017* | *0.0001* |
| Y-intercept (a) of observations versus model line | | 31.11 | **15.32** | *32.23* | ***13.59*** | ***14.2*** | ***13.17*** | ***13.17*** | *17.98* | ***15.08*** |
| Slope (b) of observations versus model line | | 0.38 | **0.70** | *0.28* | ***0.72*** | ***0.73*** | ***0.74*** | ***0.74*** | *0.66* | *0.68* |
| Correlation Coefficient (R) | | 0.58 | **0.64** | *0.53* | 0.64 | ***0.66*** | ***0.66*** | ***0.66*** | 0.64 | 0.64 |
| Mean Bias | | 17.11 | **8.48** | ***15.95*** | ***7.22*** | ***8.11*** | ***7.32*** | ***7.32*** | *10.37* | ***7.94*** |
| Mean Absolute Error | | 18.52 | **12.53** | ***18.01*** | ***12.05*** | ***12.26*** | ***11.93*** | ***11.93*** | *13.1* | ***12.22*** |
| Root Mean Square Error | | 21.25 | **16.17** | ***20.62*** | ***15.71*** | ***15.86*** | ***15.53*** | ***15.53*** | *16.78* | ***15.75*** |
| Normalized Mean Bias (%) | | 75.42 | **37.41** | ***70.32*** | ***31.84*** | ***35.75*** | ***32.26*** | ***32.26*** | *45.73* | ***35.01*** |
| Normalized Mean Error (%) | | 81.63 | **55.26** | ***79.45*** | ***53.13*** | ***54.09*** | ***52.61*** | ***52.61*** | *57.77* | ***53.89*** |



Discussion Paper | Discussion Paper | Discussion Paper | Discussion Paper |

GMDD

6, 5595–5644, 2013

Transport, emissions, & compensating errors in chemical models

P. A. Makar et al.

**Table 4.** (b) $PM_{2.5}$ statistics, Entire Grid (µg m$^{-3}$).

| $PM_{2.5}$ Statistics | OBS | CMAQ 1 Base Case | AURAMS 1 Base Case | CMAQ 2 Emissions 1 | AURAMS1b Code Improvements | AURAMS 2 Code Improvements + Emissions 1 | AURAMS 3 Code Improvements + Emissions 1, 2 | AURAMS 4 Code Improvements + Emissions 1, 2,3 | AURAMS 5 Diffusion Cut-off = 0.6 m$^2$ s$^{-1}$ | AURAMS 6 Renormalize Non-Mobile Area Sources |
|---|---|---|---|---|---|---|---|---|---|---|
| Number of Pairs | 27 236 | 27 200 | 27 236 | 27 236 | 27 236 | 27 236 | 27 236 | 27 236 | 27 236 | 27 236 |
| Mean | 7.76 | 4.70 | **10.58** | *4.08* | *10.86* | ***10.56*** | *11.39* | *11.63* | ***8.92*** | ***10.11*** |
| Maximum | 519.0 | 44.49 | **69.99** | *28.06* | ***77.3*** | ***80.87*** | ***84.07*** | ***85.34*** | *49.4* | ***68.33*** |
| Minimum | 0.0 | **1.2E-04** | 0.17 | *0.00064* | *0.2* | *0.2* | *0.21* | *0.22* | *0.22* | *0.23* |
| Y-intercept (a) of observations versus model line | | **3.64** | 7.95 | ***3.36*** | *8.1* | ***7.66*** | *8.2* | *8.35* | ***7.1*** | ***7.45*** |
| Slope (b) of observations versus model line | | 0.14 | **0.34** | *0.092* | ***0.36*** | ***0.37*** | ***0.41*** | ***0.42*** | *0.23* | 0.34 |
| Correlation Coefficient (R) | | **0.25** | 0.23 | *0.18* | 0.23 | ***0.25*** | ***0.26*** | ***0.26*** | 0.23 | ***0.24*** |
| Mean Bias | | −3.07 | **2.82** | *−3.69* | *3.1* | ***2.79*** | *3.62* | *3.87* | ***1.15*** | ***2.35*** |
| Mean Absolute Error | | **4.61** | 6.77 | *4.99* | *7.12* | 6.78 | *7.38* | *7.47* | ***5.42*** | ***6.53*** |
| Root Mean Square Error | | **7.2** | 10.53 | *7.59* | *11.07* | ***10.41*** | *11.2* | *11.36* | ***8.19*** | ***10.14*** |
| Normalized Mean Bias (%) | | −39.51 | **36.29** | *−47.51* | *39.92* | ***35.98*** | *46.66* | *49.82* | ***14.82*** | ***30.24*** |
| Normalized Mean Error (%) | | **59.33** | 87.14 | *64.3* | *91.75* | *87.35* | *95* | *96.24* | ***69.84*** | ***84.07*** |





GMDD
6, 5595–5644, 2013

Transport, emissions, & compensating errors in chemical models

P. A. Makar et al.

**Table 5.** $PM_{2.5}$ statistics, Lower Fraser Valley Stations.

| $PM_{2.5}$ Statistics | OBS | CMAQ 1 Base Case | AURAMS 1 Base Case | CMAQ 2 Emissions 1 | AURAMS1b Code Improvements | AURAMS 2 Code Improvements + Emissions 1 | AURAMS 3 Code Improvements + Emissions 1, 2 | AURAMS 4 Code Improvements + Emissions 1, 2,3 | AURAMS 5 Diffusion Cut-off = 0.6 $m^2 s^{-1}$ | AURAMS 6 Renormalize Non-Mobile Area Sources |
|---|---|---|---|---|---|---|---|---|---|---|
| Number of Pairs | 3813 | 3808 | 3813 | 3813 | 3813 | 3813 | 3813 | 3813 | 3813 | 3813 |
| Mean | 7.5 | 4.75 | **8.70** | *4.37* | ***8.43*** | ***8.27*** | 8.5 | ***8.64*** | ***7.83*** | ***7.77*** |
| Maximum | 49 | 31.95 | **53.94** | *28.06* | *58.72* | ***50.32*** | 42.86 | *40.42* | *42.42* | *35.96* |
| Minimum | 0 | **6.1E-04** | 0.52 | *6.4E-04* | ***0.44*** | ***0.5*** | 0.47 | ***0.49*** | ***0.51*** | ***0.48*** |
| Y-intercept (a) of observations versus model line | | **3.69** | 5.36 | ***3.36*** | ***5.31*** | *5.53* | 5.58 | *5.59* | ***5.18*** | ***5.22*** |
| Slope (b) of observations versus model line | | 0.14 | **0.45** | *0.13* | *0.42* | *0.37* | 0.39 | *0.41* | *0.35* | *0.34* |
| Correlation Coefficient (R) | | 0.19 | **0.28** | 0.19 | *0.27* | *0.26* | ***0.29*** | ***0.31*** | ***0.31*** | ***0.29*** |
| Mean Bias | | −2.76 | **1.2** | *−3.13* | ***0.93*** | ***0.77*** | *1* | ***1.14*** | ***0.33*** | ***0.27*** |
| Mean Absolute Error | | **4.57** | 5.28 | *4.67* | ***5.26*** | ***5.14*** | ***4.95*** | ***4.91*** | ***4.4*** | ***4.52*** |
| Root Mean Square Error | | **6.05** | 7.72 | *6.16* | ***7.62*** | ***7.19*** | ***6.82*** | ***6.74*** | ***6.06*** | ***6.20*** |
| Normalized Mean Bias (%) | | −36.73 | **15.95** | *−41.72* | ***12.38*** | ***10.23*** | *13.32* | ***15.18*** | ***4.43*** | ***3.58*** |
| Normalized Mean Error (%) | | **60.89** | 70.4 | *62.27* | ***70.06*** | ***68.59*** | ***66.05*** | ***65.42*** | ***58.69*** | ***60.23*** |



Discussion Paper | Discussion Paper | Discussion Paper | Discussion Paper |

GMDD

6, 5595–5644, 2013

Transport, emissions, & compensating errors in chemical models

P. A. Makar et al.

Title Page
Abstract Introduction
Conclusions References
Tables Figures
◀◀ ▶▶
◀ ▶
Back Close
Full Screen / Esc
Printer-friendly Version
Interactive Discussion

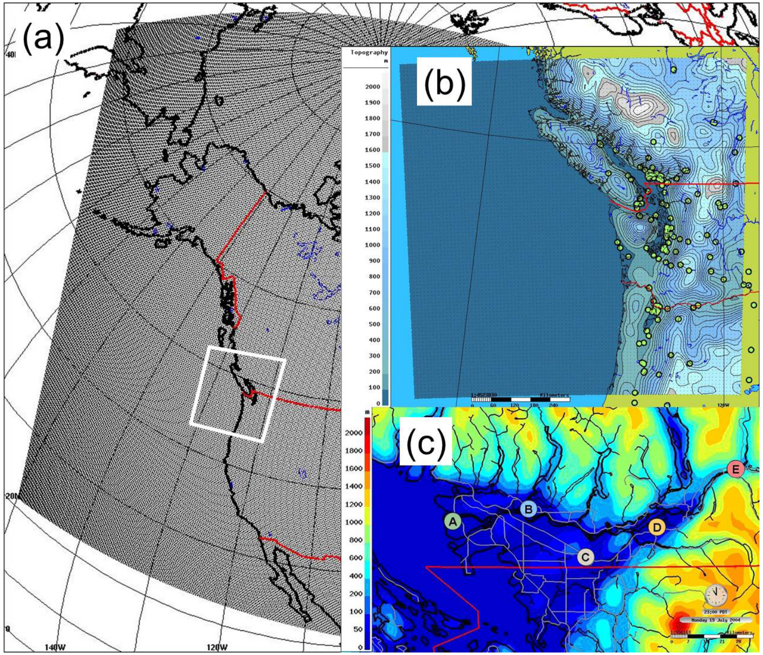


**Fig. 1. (a)** GEM 15 km domain with boundary of CMAQ and AURAMS 12 km domain shown as inset, **(b)** 12 km Pacific and Yukon Region Domain, observation stations shown as green dots, background contours elevation; **(c)** 4 stations (out of 20 total) in the Lower Fraser Valley, elevation contours.

GMDD
6, 5595–5644, 2013

Transport, emissions, & compensating errors in chemical models

P. A. Makar et al.





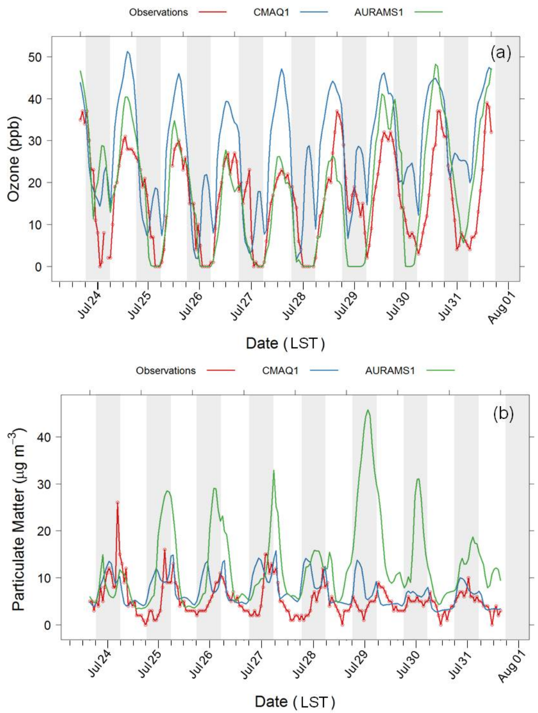


**Fig. 2.** Comparison between observations, CMAQ, and AURAMS, for **(a)** $O_3$ and **(b)** $PM_{2.5}$ at Vancouver Airport (station (A) in Fig. 1). Local standard time night (18:00 to 06:00 LST, Pacific Standard Time) shown as shaded regions.

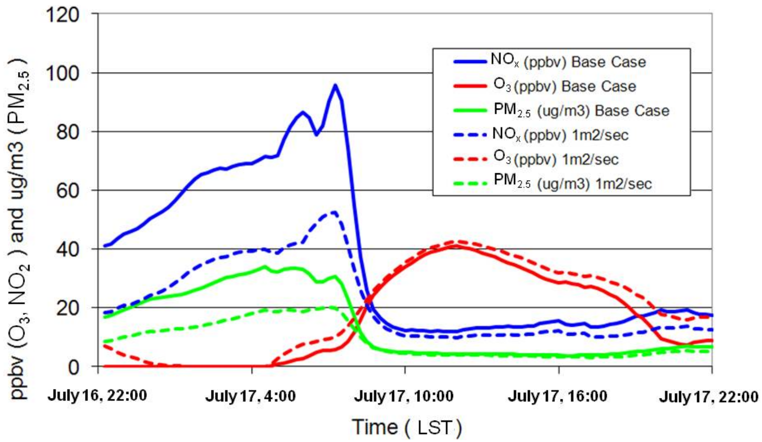


**Fig. 3.** Comparison of AURAMS results, Vancouver Airport, using default diffusion cut-off of $0.1\,m^2\,s^{-1}$ (solid lines) and CMAQ value of $1.0\,m^2\,s^{-1}$ (dashed lines).

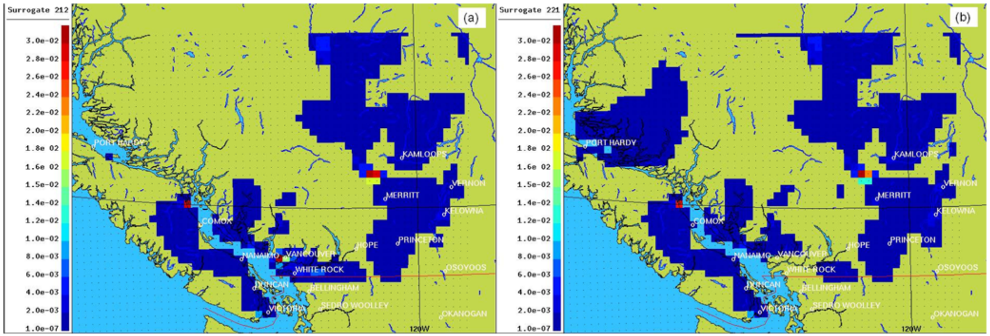


**Fig. 4.** Comparison of spatial surrogates **(a)** 212 (used previously for mining activities) and **(b)** 221 (used in Emissions 1,2,3 scenarios). Note high values of mining activity assumed in urban Vancouver in **(a)**, absent in **(b)**.

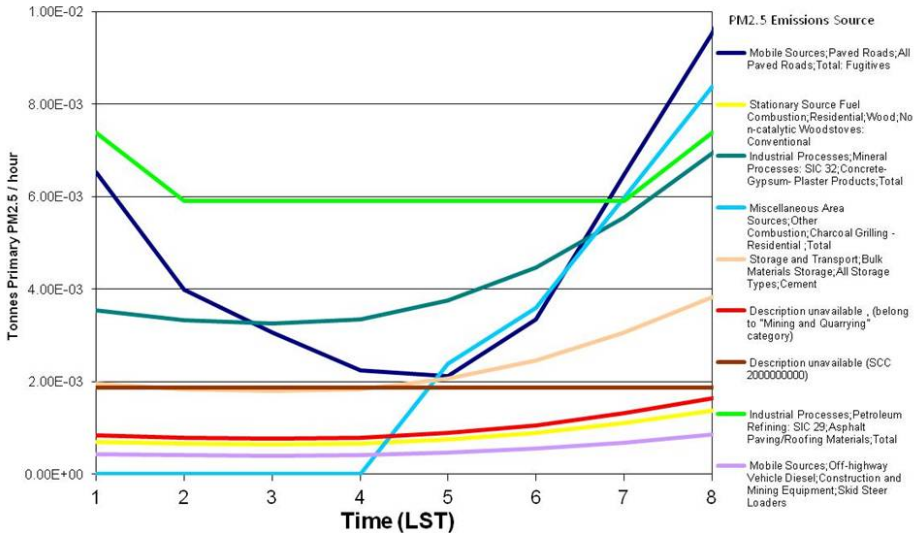


**Fig. 5.** Temporal allocation of primary $PM_{2.5}$ from top nine sources at night in Downtown Vancouver.

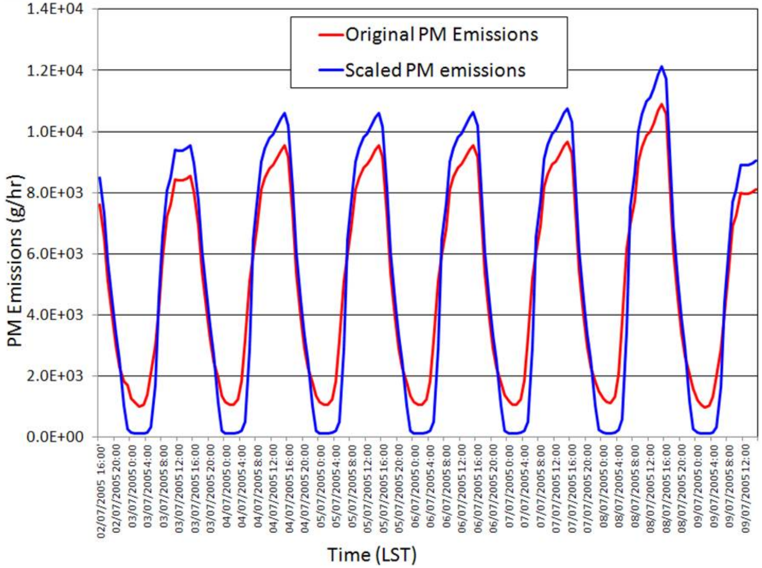


**Fig. 6.** Comparison of total PM emissions across model domain, original vs. scaled (AURAMS6 Scenario, see text).





GMDD
6, 5595–5644, 2013

Transport, emissions, & compensating errors in chemical models

P. A. Makar et al.

Title Page
Abstract | Introduction
Conclusions | References
Tables | Figures
◀| |▶
◀ ▶
Back | Close
Full Screen / Esc
Printer-friendly Version
Interactive Discussion

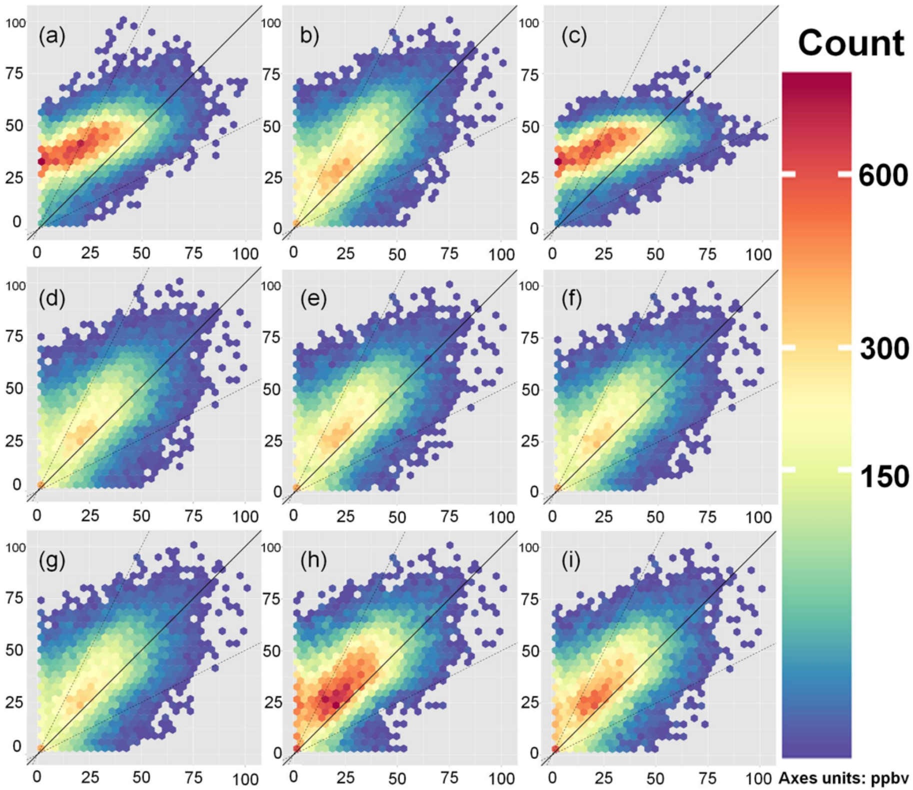


**Fig. 7.** Scatterplot hourly $O_3$ comparisons of each model run vs. observations. **(a)**, CMAQ1, **(b)** AURAMS1, **(c)** CMAQ2, **(d)** AURAMS1b, **(e)** AURAMS2, **(f)** AURAMS3, **(g)** AURAMS4, **(h)** AURAMS5, **(i)** AURAMS6. 1 : 1 line is shown as solid line, 1 : 2 and 2 : 1 lines as dotted lines. Colour bar scale is count frequency: the number of model/obs pairs falling within the given hexagon.

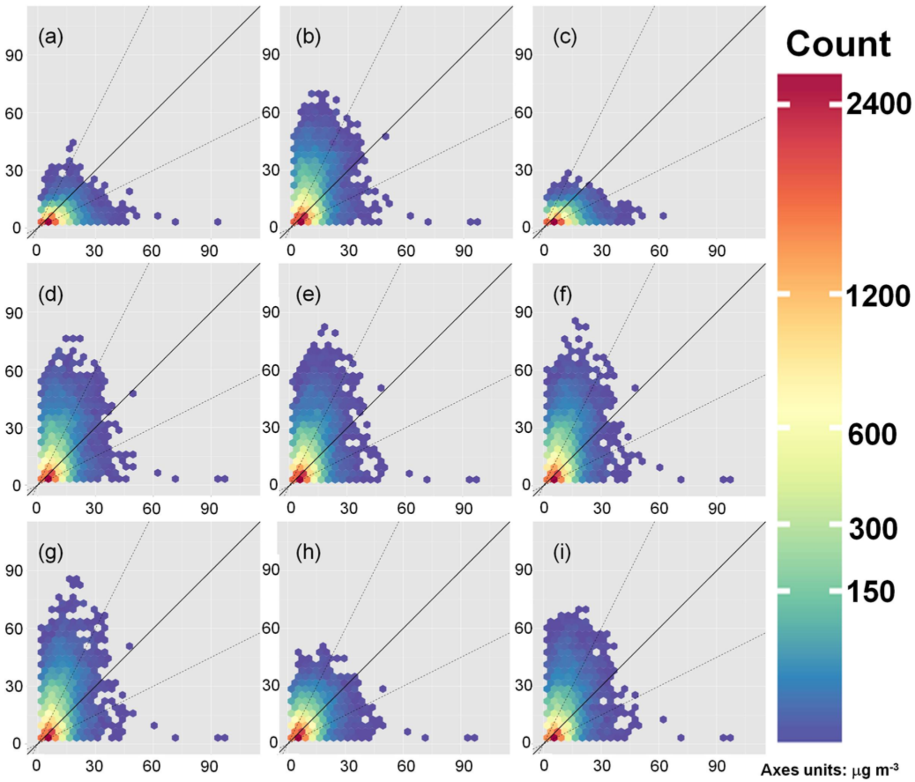


**Fig. 8.** Scatterplot hourly $PM_{2.5}$ comparisons of each model run vs. observations. **(a)**, CMAQ1, **(b)** AURAMS1, **(c)** CMAQ2, **(d)** AURAMS1b, **(e)** AURAMS2, **(f)** AURAMS3, **(g)** AURAMS4, **(h)** AURAMS5, **(i)** AURAMS6.





GMDD
6, 5595–5644, 2013



Title Page
Abstract Introduction
Conclusions References
Tables Figures
◂◂ ▸▸
◂ ▸
Back Close
Full Screen / Esc
Printer-friendly Version
Interactive Discussion

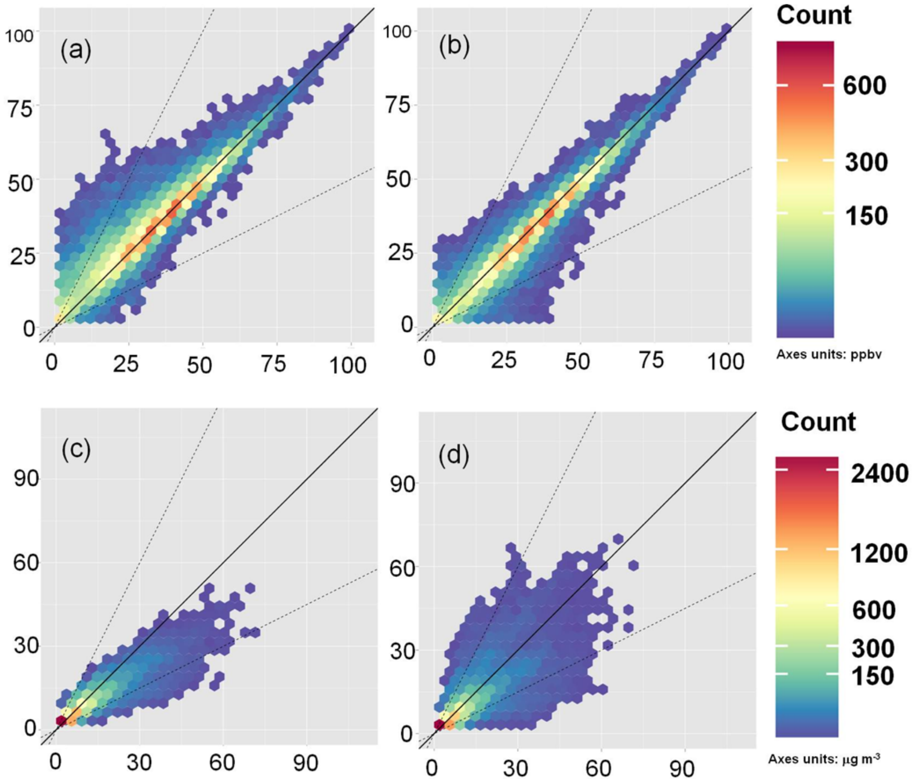


**Fig. 9.** Scatterplot comparison of $O_3$ and $PM_{2.5}$. **(a)** $O_3$, AURAMS5 vs. AURAMS1, **(b)** $O_3$, AURAMS6 vs. AURAMS1, **(c)** $PM_{2.5}$, AURAMS5 vs. AURAMS1, **(d)** $PM_{2.5}$, AURAMS6 vs. AURAMS1.





GMDD
6, 5595–5644, 2013

Transport, emissions, & compensating errors in chemical models

P. A. Makar et al.

Title Page
Abstract Introduction
Conclusions References
Tables Figures
◀| |▶
◀ ▶
Back Close
Full Screen / Esc
Printer-friendly Version
Interactive Discussion

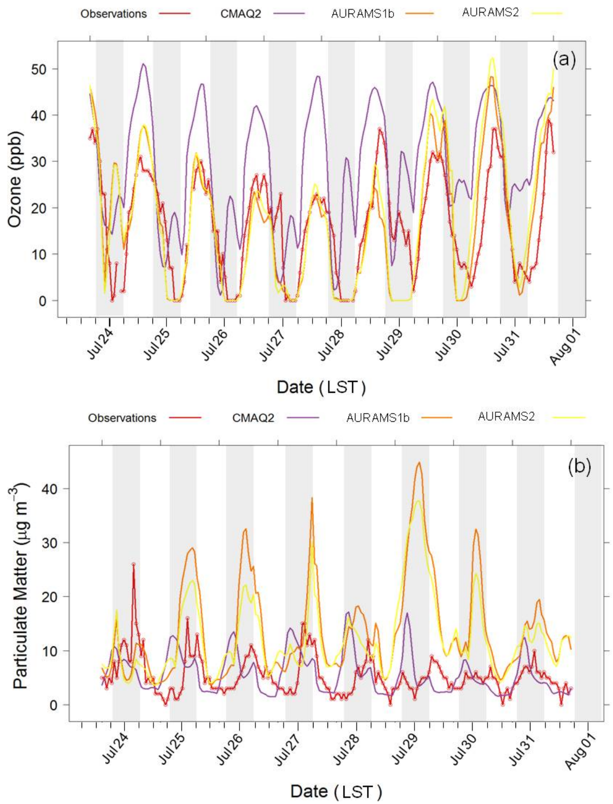


**Fig. 10.** Revised stage 1 emissions and model code compared to observations, for **(a)** $O_3$ and **(b)** $PM_{2.5}$ at Vancouver Airport. Compare to Fig. 2.

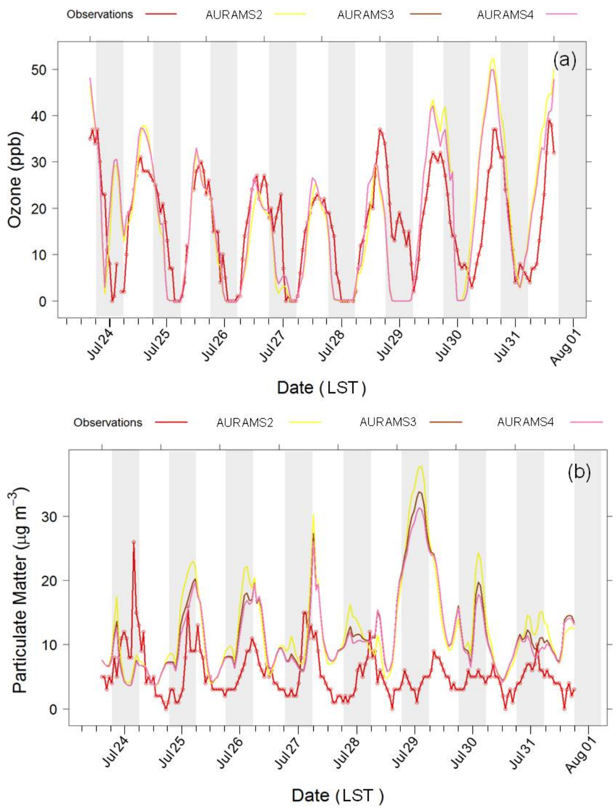


**Fig. 11.** Revised stage 1, stage 2, stage 3 emissions compared to observations, for **(a)** $O_3$ and **(b)** $PM_{2.5}$ at Vancouver Airport. Compare to Figs. 2 and 8. Note that AURAMS3 is overplotted by AURAMS4 in **(a)**.

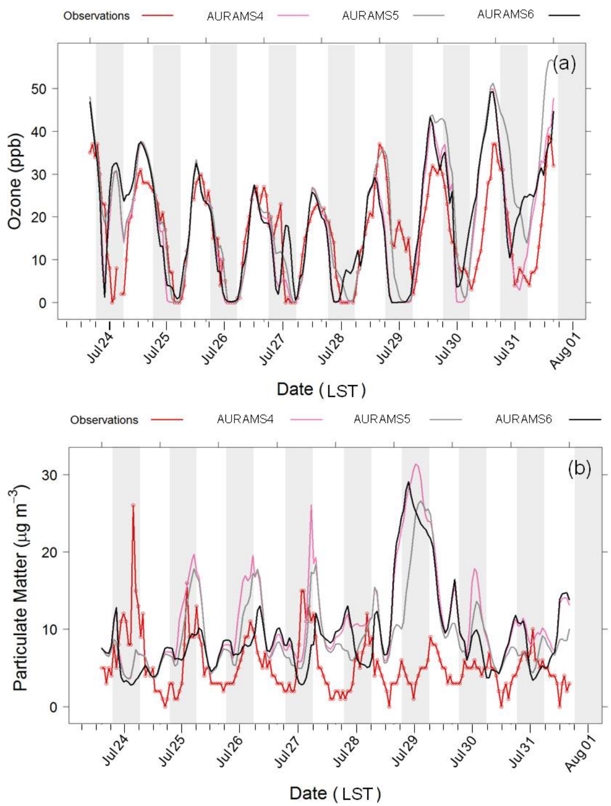


**Fig. 12.** Revised stage 3 emissions, diffusion cut-off of $0.6\,m^2\,s^{-1}$, temporally scaled non-mobile area source emissions, compared to observations at Vancouver Airport, for **(a)** $O_3$ and **(b)** $PM_{2.5}$. Compare to Figs. 2, 8 and 9.